High-T_c Ferroelectricity Emerging from Magnetic Degeneracy in Cupric Oxide

Gianluca Giovannetti,[1,2] Sanjeev Kumar,[3,4] Alessandro Stroppa,[5] Jeroen van den Brink,[3] Silvia Picozzi,[1] and José Lorenzana[2]

[1]*Consiglio Nazionale delle Ricerche CNR-SPIN L'Aquila, Italy*
[2]*ISC-CNR, Dipartimento di Fisica, Università "La Sapienza", Piazzale Aldo Moro 5, Roma, Italy*
[3]*Institute for Theoretical Solid State Physics, IFW Dresden, 01171 Dresden, Germany*
[4]*Indian Institute of Science Education and Research Mohali, MGSIPAP Complex, Sector 26, Chandigarh 160019, India*
[5]*CNISM- Department of Physics, University of L'Aquila, Via Vetoio 10, 67010 Coppito, L'Aquila, Italy*

(Received 26 July 2010; published 12 January 2011)

Cupric oxide is multiferroic at unusually high temperatures. From density functional calculations we find that the low-T magnetic phase is paraelectric, and the higher-T one is ferroelectric with a size and direction of polarization in good agreement with experiments. By mapping the *ab initio* results on to an effective spin model, we show that the system has a manifold of almost degenerate ground states. In the high-T magnetic state noncollinearity and inversion symmetry breaking stabilize each other via the Dzyaloshinskii-Moriya interaction. This leads to an unconventional mechanism for multiferroicity, with the particular property that nonmagnetic impurities enhance the effect.

DOI: 10.1103/PhysRevLett.106.026401 PACS numbers: 71.45.Gm, 71.10.Ca, 73.21.−b

The simultaneous presence of electric and magnetic ordering, known as multiferroic behavior, is particularly intriguing when the ferroelectric polarization is triggered by a specific magnetic order, as was observed for the first time by Kimura and co-workers in $TbMnO_3$ [1]. Since then, several so-called type-II multiferroics [2] have been discovered in which magnetic order causes ferroelectric order. Although plenty of potential applications are envisioned, in random access memory devices for instance, the small values of the induced polarization as well as a low transition temperature in most type-II multiferroics hinder practical applications. The very recent discovery that cupric oxide (CuO) is a type-II multiferroic with a high antiferromagnetic (AF) transition temperature T_N of 230 K changed this situation drastically and opened a possible route to room-temperature multiferroicity [3,4]. A peculiar feature of CuO is that its type-II behavior is only present at finite temperatures, between $T \sim 210$ and $T \sim 230$ K, disappearing above and below. The discovery is even more intriguing, considering that CuO is closely related to the family of copper-oxide based materials displaying High-T_c superconductivity.

In this Letter, we use a combination of density functional theory (DFT) calculations and model Hamiltonian analysis to show that multiferroicity in CuO arises via a novel mechanism in which spin canting and polarization mutually stabilize each other. Our DFT calculations for different ordered phases confirm the presence of magnetically induced ferroelectricity in CuO, with a polarization that is in close agreement with the experimental value. The *ab initio* derived magnetic Hamiltonian displays near degeneracy between polar and nonpolar states. Classical Monte Carlo simulations show that the ferroelectric phase is stabilized at finite temperatures by an unconventional mechanism involving the Dzyaloshinskii-Moriya (DM) interaction and the transverse spin-lattice coupling.

We begin by describing the results obtained within DFT [5]. In the calculations we use the experimental structure of CuO ($C2/c$ space group No. 15), where Cu ions are coordinated by 4 oxygen atoms in an approximately square-planar configuration, and form O-centered tetrahedra [6]. The low-T magnetic structure [7] (AF1 in Fig. 1) consists of Cu moments arranged ferromagnetically along x and antiferromagnetically along z, with the y axis as the easy axis. We find AF1 as the ground state, in agreement with other *ab initio* calculations [8,9]. The energy gap of 1.4 eV [10] is recovered using $U_{\text{eff}} = 5.5$ eV in GGA + U or an exact-exchange fraction $\alpha = 0.15$ in the hybrid functional approach [8].

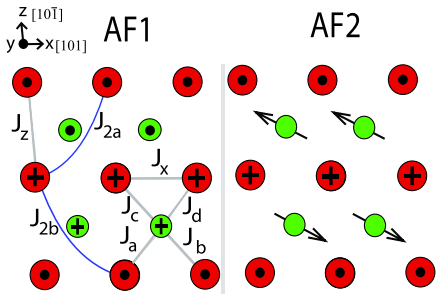

FIG. 1 (color online). Schematic view of AF1 and AF2 magnetic states. We show Cu ions belonging to different constant-y planes with big red circles ($y = 0$, termed even plane in the text) and small green circles ($y = 1/2$, termed odd plane in the text). Dot (cross) refers to spin pointing along the positive (negative) y axis.

TABLE I. Exchange coupling parameters (meV) calculated within SGGA + U and hybrid functional calculations. The structure allows for $J_a \neq J_d$ and $J_b \neq J_c$ but we take them equal for simplicity. This is inessential for our conclusions. For the notations see Fig. 1 and Ref. [8].

	J_z	J_x	J_{2a}	J_{2b}	$J_a = J_d$	$J_b = J_c$	J_y
$U_{\text{eff}} = 5.5$	107.76	−15.76	6.89	16.18	7.98	15.82	−21.48
$\alpha = 0.15$	120.42	−24.33	4.99	14.27	4.19	13.17	−23.02

We analyze the exchange interactions using the Heisenberg Hamiltonian $H_M = \sum_{ij} J_{ij} \mathbf{S}_i \cdot \mathbf{S}_j$. The parameters J_{ij}, reported in Table I, are calculated from total energy differences of several magnetic configurations within a unit cell containing 32 Cu sites. The strongest interaction $J_z \sim 100$ meV is in good agreement with optical [11] and neutron [12] experiments. Moreover, J_z is almost 5 times stronger than the next higher coupling (see Table I), in agreement with the quasi one-dimensional (1D) character reported in experiments [11–15]. The Cu and O spin moments are $0.6\mu_B$ and $0.1\mu_B$ respectively, in good agreement with neutron diffraction experiments [7].

The magnetic structure within a constant-y plane can be viewed as AF chains along z with dominant interaction J_z and moderate interchain interactions J_x, J_{2a} and J_{2b}. Hereafter, we will term the planes with $2y$ odd (even) as odd (even) planes. J_y is the ferromagnetic (FM) coupling between even and even (or odd and odd) planes separated by $\Delta y = \pm 1$. Finally, J_a, J_b, J_c and J_d are coupling between nearest neighbor (nn) planes separated by $\Delta y = \pm 1/2$. The dominant interactions determine the magnetism within a plane, which is AF along z and FM along x. Remarkably, in this configuration the energy contribution from the coupling between the nn planes vanishes. Indeed a close examination of the structure shows that the pattern of couplings between the plane at $y = 1/2$ and the plane at $y = 1$ is identical to the one of Fig. 1 but with the exchanges $J_a \leftrightarrow J_d$ and $J_c \leftrightarrow J_b$. It is easy to check that this symmetry, combined with the magnetic structure within a plane, makes the classical energy of the model independent of the relative angle between the spins on nn planes, and the ground state is infinitely degenerate. This degeneracy plays an important role in the mechanism for ferroelectricity in CuO.

Relaxation of charge and lattice, and small anisotropies favor a collinear structure. Indeed within DFT calculations, including spin-orbit (SO) coupling, we find that AF1 is the ground state with an energy gain of 2.2 meV/Cu with respect to the noncollinear AF2 structure shown in Fig. 1 and defined below. The easy axis in the collinear AF1 state is found to be along the y direction.

Experiments report an incommensurate magnetic structure with a modulation vector $Q = (0.506, 0, 0.517)$ r.l.u. in the high-T ferroelectric phase of CuO [3,7,13]. The magnetic structure within a constant-y plane is same as in the AF1, but the spins on nn planes are nearly perpendicular to each other. This is shown schematically in the right panel of Fig. 1, where the small incommensuration has been neglected. Experimentally, an electric polarization $P(\sim 0.01\ \mu\text{C/cm}^2)$ is found along the y axis [3].

On a first sight one would expect that the incommensurate spiral is crucial to obtain a finite polarization, as in the standard cycloid scenario [4,16,17]. However, the closest commensurate state to the incommensurate one (labeled AF2 in Fig. 1) has spin canting, and taking into account the SO coupling we find a polarization along y axis, in good agreement with the experiments. The electronic contribution to the polarization P was evaluated to be $P_e \sim 0.02\ \mu\text{C/cm}^2$ using the Berry phase (BP) method [18]. Thus the incommensurate state is not crucial but noncollinearity clearly is. The lattice contribution was estimated to be $P_l \sim 0.005\ \mu\text{C/cm}^2$ [19]. The perpendicular configuration ensures that AF2 state has maximal spin current (also known as vector chirality) $\mathbf{j}_{1,2} \equiv \langle \mathbf{S}_1 \times \mathbf{S}_2 \rangle$ among nn planes of different kind. We will show that this is a fingerprint of the proposed scenario.

While noncollinearity and SO coupling are standard ingredients of the cycloid mechanism [4,16,17], the situation in CuO is subtly different. We illustrate the differences and similarities between the two mechanisms using the 1D model [16] depicted in Fig. 2. Consider an hypothetical Cu-O chain with Hamiltonian $H = H_M + H_{\text{DM}} + H_E$. For the Heisenberg part, H_M, we assume a nearest neighbor AF interaction J_1 and a next nearest neighbor AF interaction J_2. The Dzyaloshinskii-Moriya (DM)[20–22] and elastic contributions read,

$$H_{\text{DM}} = \sum_n \lambda (\mathbf{u}_{n+1/2} \times \mathbf{e}_{n,n+1}) \cdot (\mathbf{S}_n \times \mathbf{S}_{n+1}),$$
$$H_E = \sum_n \frac{k}{2} |\mathbf{u}_{n+1/2}|^2. \quad (1)$$

Here, $\mathbf{u}$ are the oxygen displacements and $\mathbf{e}_{n,n+1}$ is a unit vector joining nn atoms. Assuming classical spins, for $J_2 > J_1/4$ one finds that the ground state is a spiral with pitch angle θ given by $\cos\theta = -J_1/4J_2$, and a finite spin-current

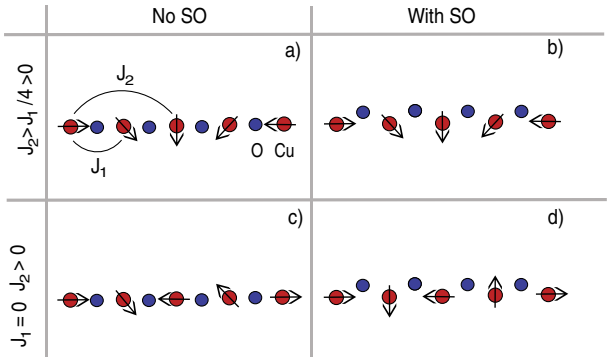

FIG. 2 (color online). Schematic mechanism of multiferroic effect in 1D. (a) and (b) standard cycloid scenario as in Ref. [16] with $J_2 > J_1/4 > 0$. (c) and (d) CuO-like mechanism with $J_1 = 0$. Without SO coupling (c) the angle between magnetic moments on nn Cu sites is undetermined. (d) SO interaction stabilizes the angle and the finite polarization.

$\mathbf{j} = \langle \mathbf{S}_n \times \mathbf{S}_{n+1} \rangle$. SO interaction is not necessary to stabilize this state [Fig. 2(a)]. In the presence of SO coupling the free energy per site due to uniform displacements u of oxygens, which are perpendicular to both the chain and to $\mathbf{j}$, is given by $\delta F_{\mathrm{DM}} = \lambda u j + \frac{k}{2} u^2$. Minimizing, one obtains a polarization $P = \delta q u = -\delta q \lambda j / k$ [Fig. 2(b)] due to the different charge $\pm \delta q$ among the two ions.

In the case $J_1 = 0$ [Figs. 2(c) and 2(d)] the system separates into two interpenetrating sublattices analogous to the odd and even planes of CuO. Without SO coupling the angle ϕ between nn spins is arbitrary and the ground state is infinitely degenerate [Fig. 2(c)]. This degeneracy can be broken by the DM interaction. The free energy per site is $\delta F = \frac{1}{2} \chi_{jj}^{-1} j^2 + \lambda u j + \frac{k}{2} u^2$. Here χ_{jj} is a spin-current susceptibility defined for H_M alone. δF has to be minimized with respect to both j and u, since H_M does not determine the spin current. Minimizing with respect to u one obtains $\delta F = \frac{1}{2} (\chi_{jj}^{-1} - \lambda^2 / k) j^2$. When

$$\chi_{jj} \frac{\lambda^2}{k} > 1 \tag{2}$$

it is convenient to maximize the spin current $j \propto \sin\phi$. Thus the energy acquires a term $\delta F \propto -\sin^2\phi$ which favors perpendicular magnetic moments on nn sites [Fig. 2(d)] analogous to the maximum spin current of CuO mentioned above. At the same time, this gives rise to a finite polarization as for the cycloid mechanism. Although the mechanism is discussed here for lattice contribution to P, it applies also for the electronic contribution which follows from the same symmetry. Note that the spontaneous breaking of symmetry and the spin canting drive each other unlike the cycloid scenario, where the spin canting is driven by the magnetic Hamiltonian. This result could have been anticipated from the work of Onoda and Nagaosa [22], which implies that the contributions in Eq. (1) can drive a sinusoidal collinear magnet into an helical magnet.

From Eq. (2) we see that the multiferroic effect is favored by strong SO coupling, soft lattices and a large spin-current susceptibility. This effect competes with thermal and quantum fluctuations which favor a collinear configuration, according to the "order-by-disorder" mechanism, and suppress χ_{jj} [23]. Also magnetostriction coupling favors a collinear state through effective biquadratic ($\sim (\mathbf{S}_i.\mathbf{S}_j)^2$) terms in the Hamiltonian [22].

The 1D mechanism discussed above can be easily generalized to CuO by replacing each magnetic site in Fig. 2 by a constant-y plane of Cu atoms shown in Fig. 1. In order to estimate χ_{jj} for the CuO structure, we perform classical Monte Carlo simulations on the following 3D spin Hamiltonian: $H = H_M + \sum_{(ij)} \mathbf{D} \cdot \mathbf{j}_{i,j}$. Here, H_M is the Heisenberg Hamiltonian with exchange parameters computed with GGA + U scheme (see Table I) and the second term describes the linear coupling of the spin-current between nn planes to an auxiliary external field $\mathbf{D}$. Summation index (ij) represents bonds indicated as J_a, J_b, J_c, and J_d in Fig. 1. We take $\mathbf{D}$ directed along the x axis for all pairs in the unit cell. Rather than measuring the spin current, we compute the sum of the relevant components which is proportional to the polarization, $\mathbf{p} = \sum \mathbf{e}_{ij} \times \langle \mathbf{S}_i \times \mathbf{S}_j \rangle$. The desired susceptibility is given by $\chi_{jj} = p_y / D_x$ in the limit of vanishing D_x. When χ_{jj} is large and the condition Eq. (2) is satisfied a spontaneous D and polarization stabilize each other as explained above. Notice that D breaks inversion symmetry in the system whereas the high temperature structure of CuO has inversion so there is no "permanent" D in the high temperature phase. Of course there will be DM couplings at high-temperatures in the CuO structure, but those preserve inversion symmetry and are not related to the appearance of the polarization. For simplicity we neglect these latter couplings.

To lift the degeneracy between AF1 and AF2 in favor of the former we introduce a weak anisotropy in the Heisenberg exchange term. This is done by replacing $J_z \mathbf{S}_i \cdot \mathbf{S}_j$ by $J_z (S_i^x S_j^x + (1+\gamma) S_i^y S_j^y + S_i^z S_j^z)$ in H_M. Other small terms like the biquadratic contribution are expected to have a similar effect. We use $\gamma = 0.02$ which translates into an anisotropy energy of $\sim \gamma J_z = 2.15$ meV.

We employ a classical Monte Carlo (MC) technique to explore the competition between different magnetic states at zero and finite temperatures. Given that the CuO is a system with spin $1/2$, the quantum effects in this system are unavoidable. Nevertheless the interesting transitions occur at high temperatures where it is safe to assume a classical renormalized regime [24]. In order to simplify the Monte Carlo computation we consider only 4 possible states at 90° for the spin variables. Figure 3(a) shows the phase diagram in the T-D plane. In the absence of the external field D, the system undergoes a transition from a paramagnetic (PM) to an AF1 state with $T_N \sim 250$ K. Presence of a small D opens a narrow window near T_N where AF2 is stabilized. A large external field ($D > \gamma J_z / 8 \sim 0.27$ meV at $T = 0$) eventually drives the

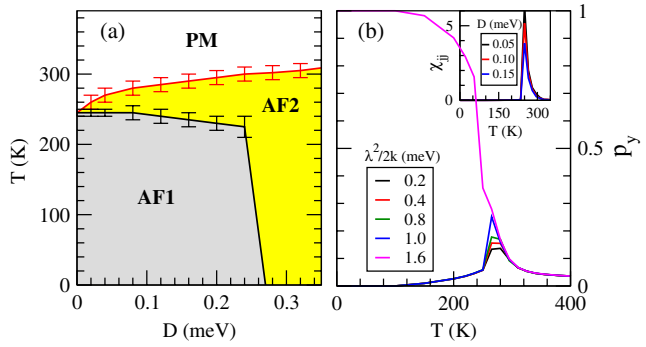

FIG. 3 (color online). (a) Phase diagram of the magnetic model of CuO with an external field coupling linearly with the spin current. (b) Polarization of the CuO model with the addition of a biquadratic spin-current term obtained by eliminating the lattice degrees of freedom in the DM coupling. Curves are labeled by the value of $\lambda^2/(2k)$. The inset shows the susceptibility computed as p_y/D. Within linear response one should take the limit $D \to 0$ corresponding to the upper curves.

ground tstate to be AF2. The inset of Fig. 3(b) shows the susceptibility computed as the ratio p_y/D_x for small D_x. Remarkably a strong peak appears around the PM to AF1 transition which will favor a spontaneous polarization of the system.

In order to test the mechanism, we again consider the 3D CuO model with the terms H_{DM} and H_E analogous to the 1D model. The lattice displacements are integrated out leading to a quadratic effective interaction among spin currents Therefore, $H_{\mathrm{DM}} + H_E$ is replaced by $H_{\mathrm{DME}} = -(\lambda^2/2k)\sum_{(ij)}(\mathbf{S}_i \times \mathbf{S}_j)^2$. Figure 3(b) shows the spontaneous polarization p as a function of temperature for the model defined by $H = H_M + H_{\mathrm{DME}}$. As expected one finds that, close to the PM to AF1 transition, H_{DME} induces a phase with broken inversion symmetry and a spontaneous polarization as seen in the experiment. The peak in the polarization is very similar to the experimental observations of a finite electrical polarization between 230 and 213 K [3]. If $\lambda^2/(2k)$ is made too large (> 1 meV) the ferroelectric phase extends down to zero T.

Our Monte Carlo simulations suggest that, the origin of spontaneous polarization lies in a strong enhancement of spin-current susceptibility close to the AF1-PM transition. While there is, of course, a divergent staggered susceptibility when approaching the AF1-PM phase transition, the enhancement of the unrelated spin-current susceptibility is non trivial. This is similar to the physics of quantum critical points relevant to heavy fermion compounds [25] where close to the quantum transition between a disordered and a magnetically ordered state, a different order (superconductivity) appears, which can be attributed to an enhanced pairing susceptibility.

As mentioned above, thermal and quantum fluctuations tend to suppress χ_{jj} and the polarization. On the other hand, disorder on the magnitude of the magnetic moments will enhance the tendency to have perpendicular orientations of spins on nn planes and hence the polarization [23]. Nonmagnetic impurities, vacancies or magnetic impurities with a different spin will lead to this effect. This opens a new way to engineer high-T_c multiferroic materials. In addition our results suggest a recipe to discover new manipulable multiferroics, i.e., to search for other materials where two magnetic subsystems have negligible interactions by symmetry but strong interactions within one subsystem.

To summarize, our density functional calculations confirm the magnetically induced ferroelectricity in CuO with polarization in agreement with experiments. By combining Monte Carlo analysis with the exchange constants derived by *ab initio* simulations we also confirm the high T_N of this compound. We explain the multiferroic effect as arising from an unconventional mechanism in which spin canting and polarization mutually stabilize each other with a crucial role of DM interaction and transverse spin-lattice coupling. Our results open new routes for the material design of multiferroics.

This work is supported by the European Research Council through the BISMUTH project (Grant N. 203523), IIT-Seed project NEWDFESCM and by CINECA and CASPUR. We thank A. Boothroyd for a critical reading of the manuscript.

Note added.—During the completion of this manuscript we became aware of Ref. [26], presenting results from *ab initio* calculations similar to ours. The mechanism for multiferroicity that we present here, however, is very different from the findings in Ref. [26].

[1] T. Kimura *et al.*, Nature (London) **426**, 55 (2003).
[2] J. van den Brink and D. Khomskii, J. Phys. Condens. Matter **20**, 434217 (2008).
[3] T. Kimura *et al.*, Nature Mater. **7**, 291 (2008).
[4] M. Mostovoy, Nature Mater. **7**, 269 (2008).
[5] We have used the PAW method as implemented in VASP, G. Kresse and J. Furthmuller, Comput. Mater. Sci. **6**, 15 (1996). To take into account the Coulomb interactions between the Cu 3*d* electrons we employ SGGA + U [27] and hybrid functional (HSE) [28] schemes.
[6] S. Asbrink *et al.*, Acta Crystallogr. Sect. B **26**, 8 (1970).
[7] J. B. Forsyth *et al.*, J. Phys. C **21**, 2917 (1988).
[8] X. Rocquefelte *et al.*, J. Phys. Condens. Matter **22**, 045502 (2010).
[9] A. Filippetti and V. Fiorentini, Phys. Rev. Lett. **95**, 086405 (2005).
[10] J. Ghijsen *et al.*, Phys. Rev. B **38**, 11322 (1988).
[11] S. H. Jung *et al.*, Phys. Rev. B **80**, 140516 (2009).
[12] Boothroyd *et al.*, Physica (Amsterdam) **234–236B**, 731 (1997).
[13] B. X. Yang, J. M. Tranquada, and G. Shirane, Phys. Rev. B **38**, 174 (1988); B. X. Yang *et al.*, Phys. Rev. B**39**, 4343 (1989).
[14] M. Aïn *et al.*, Physica (Amsterdam) **162–164C**, 1279 (1989).
[15] T. Shimizu *et al.*, Phys. Rev. B **68**, 224433 (2003).
[16] S. W. Cheong *et al.*, Nature Mater. **6**, 13 (2007).
[17] M. Kenzelmann *et al.*, Phys. Rev. Lett. **95**, 087206 (2005).
[18] R. D. King-Smith and D. Vanderbilt, Phys. Rev. B **47**, 1651 (1993).
[19] G. Giovannetti *et al.*, Phys. Rev. Lett. **103**, 266401 (2009).
[20] I. Dzyaloshinskii, J. Phys. Chem. Solids **4**, 241 (1958).
[21] T. Moriya, Phys. Rev. **120**, 91 (1960).
[22] S. Onoda and N. Nagaosa, Phys. Rev. Lett. **99**, 027206 (2007).
[23] C. L. Henley, Phys. Rev. Lett. **62**, 2056 (1989).
[24] S. Chakravarty, B. I. Halperin, and D. R. Nelson, Phys. Rev. B **39**, 2344 (1989).
[25] P. Monthoux, D. Pines, and G. G. Lonzarich, Nature (London) **450**, 1177 (2007).
[26] Guangxi Jin, Kun Cao, Guang-Can Guo, and Lixin He, arXiv:1007.2274.
[27] J. P. Perdew *et al.*, Phys. Rev. B **46**, 6671 (1992); **48**, 4978 (1993); A. Rohrbach, J. Hafner, and G. Kresse, *ibid.* **69**, 075413 (2004); Dudarev *et al.*, *ibid.* **57**, 1505 (1998).
[28] J. Heyd *et al.*, J. Chem. Phys. **118**, 8207 (2003); J. Heyd *et al.*, J. Chem. Phys. **124**, 219906 (2006).